Check for updates

A renewable tung oil-derived nitrile rubber and its potential use in epoxy-toughening modifiers†

Laihui Xiao, [ID] [ab] Zengshe Liu,[c] Fangfang Hu,[ab] Yigang Wang,[a] Jinrui Huang, [ID] [a] Jie Chen[a] and Xiaoan Nie*[a]

In this study, a modifier (CTMA) prepared by emulsion copolymerization of tung oil fatty acid, methyl esters of tung oil fatty acid and acrylonitrile was used to toughen epoxy resins. The structural characterization of the copolymer was carried out by Fourier transform infrared spectroscopy, ^{1}H NMR spectroscopy and high-temperature gel permeation chromatography. Mechanical testing, thermal characterization and scanning electron microscopy were conducted to investigate the properties of epoxy resin modified by the copolymer and further reveal its toughening mechanism. The results indicated that the newly synthesized copolymer effectively toughened the epoxy resin because the elongation-at-break was increased to 89.48%, the maximum toughness calculated by work before break was nearly 4.6 times that of the neat epoxy resin, and apparent shear yields and plastic deformations were observed in the morphology of the fractured surfaces. CTMA, which acts as a flexible cross-linker in the epoxy thermoset, may decrease the cross-linking density.

Introduction

Epoxy resins are widely used in materials science, engineering and industry because of their excellent mechanical properties, low cure shrinkage, excellent cohesiveness and good chemical resistance. However, the high cross-linking structure of epoxy resins is responsible for their poor fracture toughness.[1] To overcome this drawback, modifiers are incorporated into the epoxy curing system.

Many kinds of modified resins, such as rubbers, thermoplastic particles, core–shell polymers and hyperbranched polymers, have been used to improve the flexibility of epoxy resins. Acting as stress concentrators, the modifiers in epoxy matrices terminate cracks by different mechanisms such as multiple crazing mechanism, multiple shear yielding mechanism, multiple crazing with multiple shear yielding mechanism and cavitation mechanism.[2–5] However, because of the reaction-induced mechanism, the generation of phase separation depends on the choice of epoxy resin, curing agent and processing conditions. Therefore, a curing system toughened by modified resins will not always induce phase separation.[6–9]

Among the rubbers used as modifiers, the carboxyl-terminated copolymer of acrylonitrile and butadiene (CTBN) has been extensively used. The chemical reaction between carboxyl and epoxy groups is able to improve the compatibility between CTBN and epoxy resin, and the long flexible chains may toughen epoxy matrices by developing stress concentrations under stress.[10–12] Laura *et al.* have studied CTBN-modified epoxy resin by laser confocal microscopy characterization and found that the fracture toughness increases, whereas the glass transition temperature and the tensile modulus decrease as the size and phase volume of CTBN increase;[13] Huang *et al.* have prepared a flexible and transparent epoxy resin with tunable mechanical properties by the reaction between hydrazine hydrate and the epoxy functional group diglycidyl ether of bisphenol A (DGEBA). The curing systems incorporated with the modified resin demonstrated excellent flexibility; however, no phase separation was observed.[14] Day *et al.* have toughened epoxy resin with a series of multilayer core–shell particles. Compared to acrylic toughening particles (ATP) and CTBN under the same conditions, the epoxy resin modified by these multilayer core–shell particles improved the toughness, which led to a significant decrease in Young's modulus.[15] Fei *et al.* used hyperbranched polymers to toughen the epoxy resin that were synthesized from the diglycidyl ether of bisphenol A, succinic acid (SA) and 1,3,5-benzenetricarboxylic acid (BA). After being cured by methylhexahydrophthalic anhydride (MeHHPA), the modified epoxy thermosets exhibited better toughness as the elongation-at-break of 5.25% could be achieved as

[a]Institute of Chemical Industry of Forestry Products, CAF, National Engineering Lab for Biomass Chemical Utilization, Key Lab on Forest Chemical Engineering, SFA, Key Lab of Biomass Energy and Material, Nanjing, Jiangsu 210042, PR China. E-mail: niexiaoan@126.com; Tel: +86-025-8548-2528

[b]Co-Innovation Center of Efficient Processing and Utilization of Forest Resources, Nanjing Forestry University, China

[c]USDA, ARS, National Center for Agricultural Utilization Research, Bio-Oils Research Unit, 1815 N University St, Peoria, IL, 61604, USA

† Mention of trade names or commercial products in this publication is solely for the purpose of providing specific information and does not imply recommendation or endorsement by the U.S. Department of Agriculture. USDA is an equal opportunity provider and employer.

Paper

compared to 3% of the neat epoxy thermoset; in addition, the glass transition temperatures of the modified epoxy thermosets increased because of their hyperbranched structure.[8]

However, due to the growing concerns over sustainability and environmental friendliness, the use of renewable materials is necessary; therefore, traditional methods of toughening the epoxy resin by petroleum-based modified resins are being gradually replaced by those involving the use of renewable materials. Thus, the synthesis of modifiers partly or completely from renewable feedstock is urgent.

Vegetable oils (VOs) are excellent alternatives due to their abundance, low price and biodegradability.[16,17] Many studies have been devoted towards the toughening of epoxy resin by epoxidized vegetable oils.[18,19] These epoxidized vegetable oils are incorporated into epoxy thermosets as a flexible cross-linker, which toughen the epoxy resin by decreasing the cross-linking density. Ratna *et al.* toughened DGEBA by epoxidized soybean oil using an ambient-temperature hardener. When the addition amount of the modifier was increased from 5% to 30%, the maximum elongation-at-break obtained was 7.5% (which was 3.2% for the sample without the modifier); this led to a significant improvement in toughness;[20] however, it still could not satisfy the requirement for application in certain special occasions.

Moreover, the conjugated structure in tung oil obtained *via* the Diels–Alder reaction rather than epoxidization has received significant research interest. By the Diels–Alder reaction, a number of tung oil-derived toughened epoxy resins have been produced.[21–24] As is well-known, the products obtained *via* the Diels–Alder reaction contain a ring structure, which may reduce the toughening effect. Hence, to avoid the formation of a ring structure, an alternative strategy is to synthesize the tung oil-based toughener *via* radical polymerization; however, only few studies have been reported on the synthesis of an epoxy resin toughener by the radical polymerization of tung oil or tung oil-derives.

In this study, a renewable toughener was synthesized by the emulsion polymerization of tung oil fatty acid (TOFA), methyl esters of tung oil fatty acid (METOFA) and acrylonitrile. The long flexible aliphatic chains of tung oil-derives were able to toughen the rigid epoxy matrix, and the carboxyl groups of TOFA improved the compatibility of blends. Then, to study the effect of the addition content of the synthesized resin on the properties of the modified epoxy resin, the synthesized resin in different contents was incorporated into the epoxy matrix by a pre-reaction between the carboxyl groups and epoxy groups. After curing, the mechanical properties and thermal characterizations were investigated by mechanical testing, differential scanning calorimetry (DSC), dynamic mechanical analysis (DMA) and thermogravimetric analysis (TGA). In addition, the fracture surfaces were observed by a scanning electron microscope (SEM). The results of this study show that the synthesized copolymer resin can effectively toughen the epoxy resin.

Experimental

Material

Tung oil was obtained from the Institute of Chemical Industry of Forestry Products. Diglycidyl ether of bisphenol A (epoxide value: 0.48–0.54 equiv. $(100 \text{ g})^{-1}$), Baling Petrochemical Branch Company, PetroChina Co., Ltd, polyetherimide (D230, amine value: 8.1–8.7 mequiv. g^{-1}, Huntsman Chemical Co., Ltd), triphenylphosphine (99.5%, Shanghai Lingfeng Chemical Reagent Co., Ltd), acrylonitrile (98%, Sinopec Shanghai Petrochemical Co., Ltd), potassium oleate (98%, Shanghai Macklin Biochemical Co., Ltd), ammonium persulphate (98%, Shanghai Lingfeng Chemical Reagent Co., Ltd), sodium chloride (Xilong Scientific Co., Ltd), sodium hydroxide (Xilong Scientific Co., Ltd), potassium hydroxide (Xilong Scientific Co., Ltd), methanol (99.5%, Nanjing Chemical Reagent Co., Ltd), hydrochloric acid (36.0–38.0%, Nanjing Chemical Reagent Co., Ltd) and epoxidized soybean oil (epoxide value: 0.38 equiv. $(100 \text{ g})^{-1}$, Shanghai Aladdin Chemical Reagent Co., Ltd) were used as received.

Synthesis

Tung oil fatty acids (TOFA). Tung oil (180 g) and NaOH solution (100 mL) prepared by dissolving 24 g of sodium hydroxide in 100 mL water/ethanol (1 : 1 v/v) were taken in a flask, followed by refluxing for 3 h at 75 °C. After decomposing the soaps by hydrochloric acid, the water layer was removed. The crude product was rinsed with water, and the trace amount of water was removed by a rotary evaporator under vacuum at 70 °C. Then, 161 g of a light brown product was obtained, whose acid value was 200.3 mg g^{-1} (theoretical: 201.8 mg g^{-1}).

Methyl esters of tung oil fatty acids (METOFA). Tung oil (200 g), methanol (54 g) and potassium hydroxide (3 g) were charged into a three-necked flask fitted with a mechanical stirrer and refluxed at 70 °C for 1.5 h. After the excess methanol was removed using a rotary evaporator under vacuum, the product was easily separated from the reaction mixture. The purification methods are the same as those used for TOFA, and 187 g of a yellow product was obtained.

Copolymer of tung oil fatty acids, methyl esters of tung oil fatty acids and acrylonitrile (CTMA). TOFA (15 g), METOFA (15 g), acrylonitrile (20 g), potassium oleate (0.5 g) and water (100 g) were charged into a round-bottomed flask fitted with a magnetic stirrer and a condenser. Under a nitrogen atmosphere, the reaction system was heated to 70 °C, and ammonium persulphate (0.4 g ammonium persulphate was dissolved in 20 g water beforehand) was added to the mixture. After stirring at 70 °C for 10 h, the product was agglomerated by adding NaCl (10 g). The crude product was purified by acetone and water and dried under vacuum at 75 °C. Then, 36.8 g of a viscous product was obtained.

The preparation method is shown in Fig. 1.

Preparation of the CTMA-toughened epoxy resin (E-CTMA) and curing procedure

Epoxy resin and CTMA (in the mass ratios of 100 : 25, 100 : 35, and 100 : 45) were charged into a flask. After catalysis by
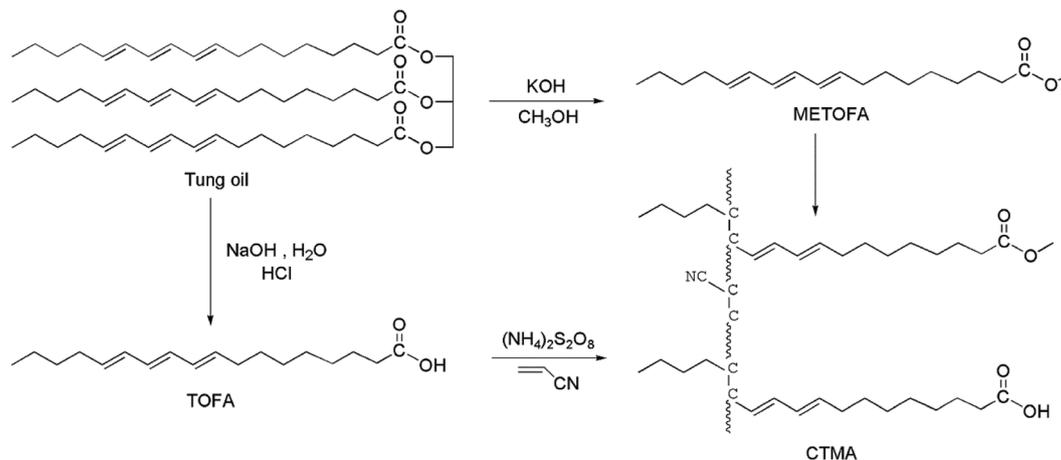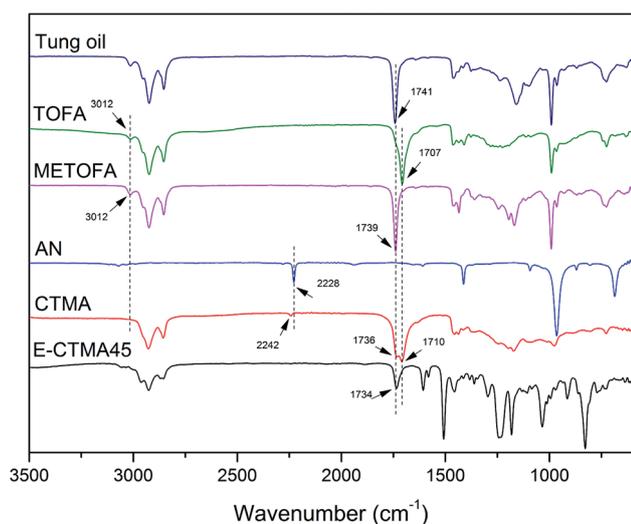
Fig. 1 Synthesis routes of CTMA.

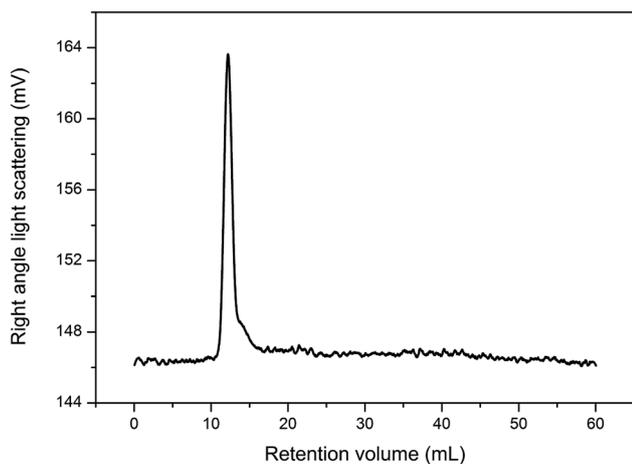Fig. 2 FTIR spectra of CTMA and materials.

Fig. 3 GPC spectrum of CTMA.

triphenylphosphine (0.2 wt% of epoxy resin), the mixture was stirred at 130 °C for 3 h. After the product was cooled down to room temperature, polyetherimide was added (epoxy and curing agent were in the 1 : 1 equivalent ratio). The mixture was then charged into a stainless mold preheated at 80 °C. Curing was performed at 40 °C for 24 h and at 80 °C for 3 h. These samples were then coded as E-CTMA25, E-CTMA35 and E-CTMA45. Epoxidized soybean oil (ESO) was blended with epoxy resin in the mass ratio of 100 : 45 at room temperature, and the sample was coded as E-ESO45, which was then used for comparison purposes. Neat epoxy resin (EP) was also prepared in the same way as a control group.

Characterization

Structural characterization. Fourier transform infrared (FTIR) analysis was performed using the Thermo Scientific Nicolet iS10 spectrometer in the wavenumber range of 600–4000 cm^{-1}. The ^{1}H NMR spectra of tung oil-derives and CTMA were obtained by the Bruker 400 MHz spectrometer at room temperature using deuterated chloroform (CDCl$_3$) as a solvent. The number-average molecular weight (M_n) and dispersity ($Đ$) were determined using the Viscotek model 350 high-temperature gel permeation chromatograph (HTGPC) at 60 °C with N,N-dimethylformamide (DMF) as the solvent. The flow rate was 1 mL min^{-1}, and the detector was right angle scattered light, whose temperature was 60 °C.

Thermal characterization. Differential scanning calorimetry (DSC) was conducted using a Diamond DSC (PE) instrument. The samples 5–10 mg in weight were placed in aluminum pans under a nitrogen atmosphere. After being heated from −50 °C to 180 °C at 10 °C min^{-1} and maintained isothermally for 5 min to eliminate the thermal history, the samples E-CTMAs and neat epoxy resin were cooled down to −50 °C and reheated to 180 °C under the same conditions. The operations for the sample CTMA were the same as those used for E-CTMAs, except that the temperature range was from −70 °C to 80 °C. Moreover, the curing behaviour was studied by DSC, and all samples were scanned from 0 °C to
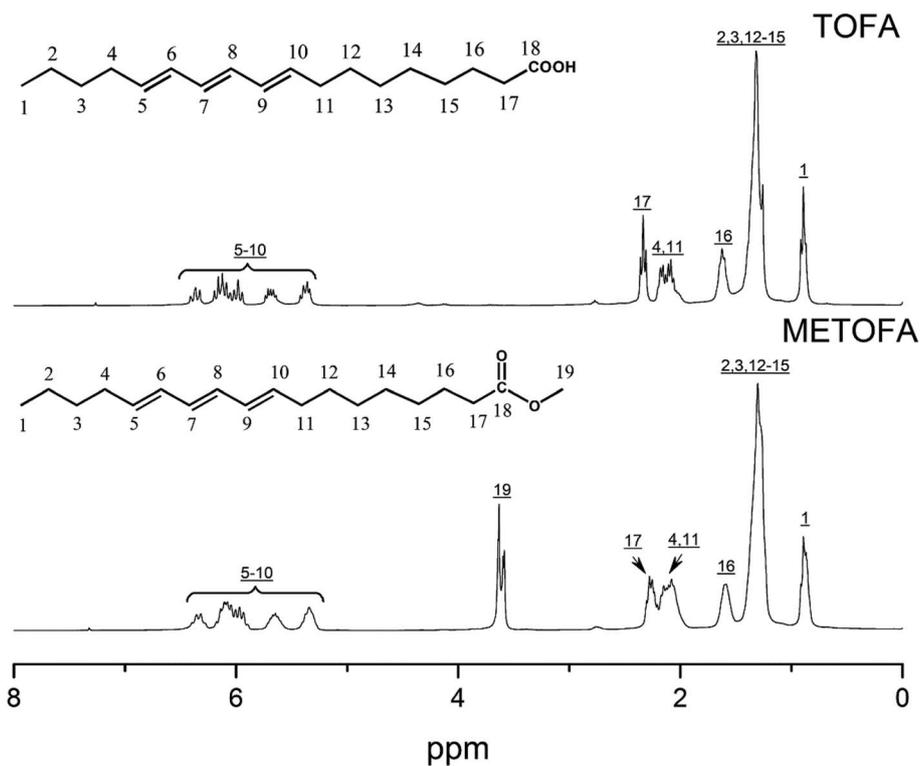
Fig. 4 ^{1}H NMR spectra of TOFA and METOFA.

250 °C at 10 °C min^{-1}. Dynamic mechanical analysis (DMA) of the samples was performed by DMA Q800 (TA Instruments) in the dual cantilever mode with the oscillating frequency of 1 Hz. The temperature range from −50 °C to 150 °C at 3 °C min^{-1} was used. Thermogravimetric analysis (TGA) was performed using the TG209F1 TGA (Netzsch) instrument. Each sample was scanned from 30 °C to 800 °C at 20 °C min^{-1} under a nitrogen atmosphere.
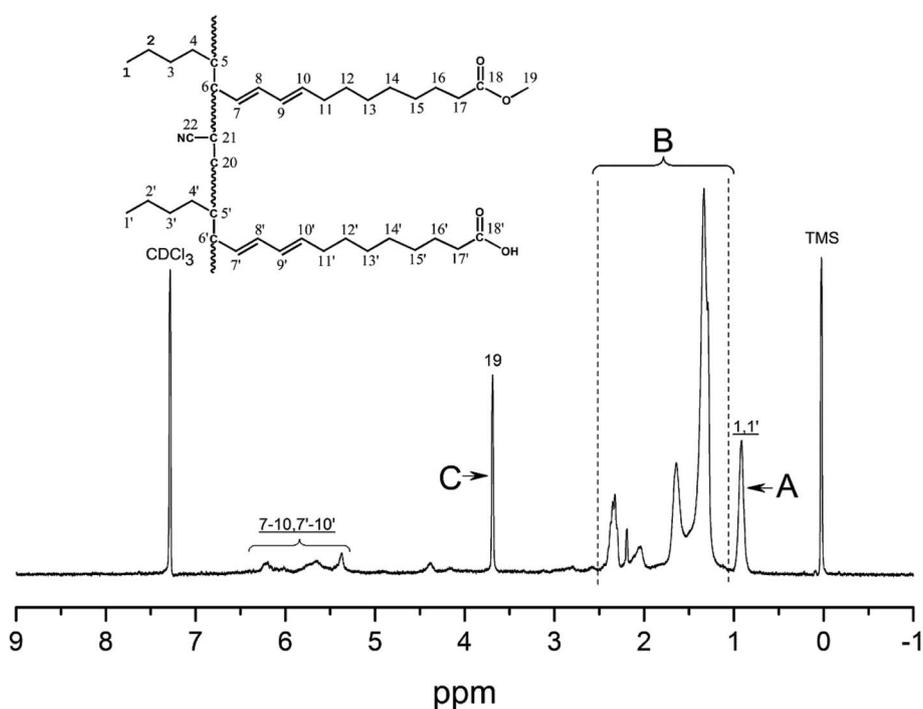

Fig. 5 ^{1}H NMR spectrum of CTMA.

Table 1 Calculation results obtained by the ^{1}H NMR spectra

| Part	A	B	C
Peak area (relative to C)	1.75	14.28	1
Monomer	AN	METOFA	TOFA
Mole fraction (%)	45.26	31.28	24.06

Scanning electron microscopy characterization. Surface morphology of the samples was determined using the 3400 NI scanning electron microscope (Hitachi) at the acceleration voltage of 15 kV. All samples were fractured after being placed in liquid nitrogen and coated with gold before examination.

Mechanical properties. Tensile tests were conducted using the Instron 4201 machine equipped with a 30 kN electronic load cell according to the Chinese standard GB13022-91. Moreover, five replicates for each sample were tested at the crosshead speed of 5 mm min^{-1} at 25 °C.
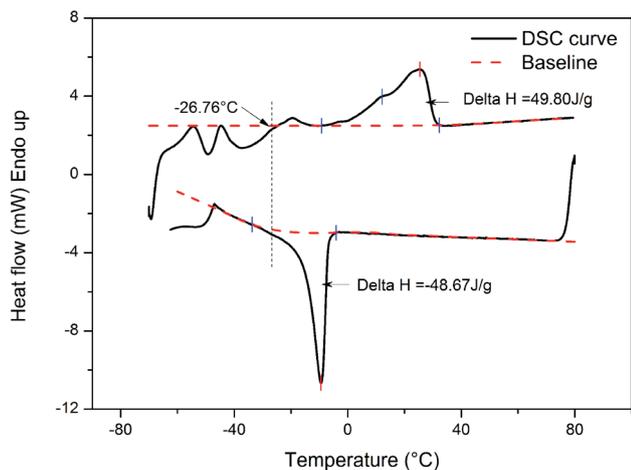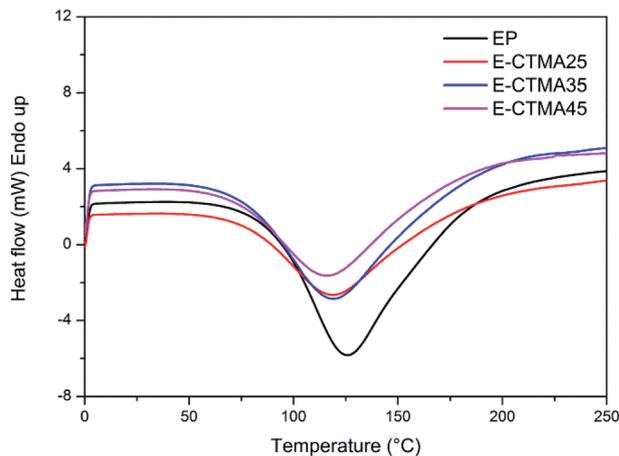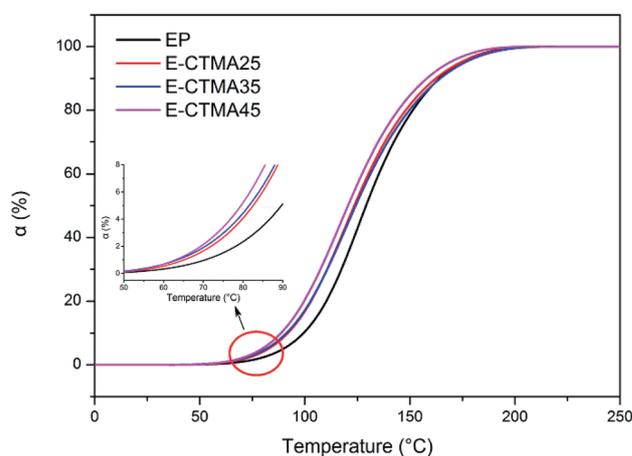

(a)
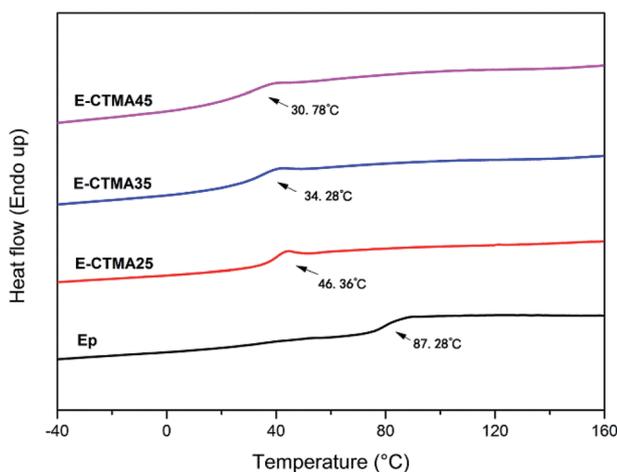
(b)

Fig. 6 DSC curves of CTMA (a) and cured thermosets (b).

(a)

(b)

Fig. 7 DSC curves of the curing process: heat flow against temperature (a) and conversion against temperature (b).

Results and discussion

Structure determinations

As shown in Fig. 2, functional group conversion can be detected by comparing the infrared spectra. In the CTMA spectrum, a weaker peak of =C–H appeared at 3012 cm^{-1} as compared to that of tung oil-derives, which indicated the polymerization of

Table 2 Curing parameters and viscosity of samples

Sample	$T_o{}^a$ (°C)	$T_p{}^b$ (°C)	ΔH (J g^{-1})	Viscosity^c (kPa s)
EP	89.17	126.18	379.65	12.36
E-CTMA25	78.37	119.43	297.89	19.16
E-CTMA35	77.89	119.25	292.83	27.08
E-CTMA45	74.43	116.78	244.34	51.22

^{a} T_o is the initial curing temperature. ^{b} T_p is the temperature at which the curing rate is maximum. ^{c} Viscosity is measured at room temperature.

the double bond. Furthermore, the peaks of –COOCH$_3$ at 1739 cm^{-1}, –COOH at 1707 cm^{-1} and –CN at 2228 cm^{-1} were observed in the CTMA spectrum, indicating that CTMA contained these three monomer units. Due to the reaction between the carboxyl groups and the epoxy groups, the peak of –COOH at 1707 cm^{-1} disappeared in the spectrum of E-CTMA45.

Fig. 3 shows the GPC spectrum of CTMA. Only one peak was observed in the spectrum, which confirmed that the main product was the copolymer of the three monomer units. The number-average molecular weight is about 28 740 g mol^{-1}, and the Đ value is 5.43. The high Đ value may be attributed to the different monomer activities of acrylonitrile and tung oil-derives. Furthermore, the simultaneous addition of monomers contributed to high Đ value.

Fig. 4 and 5 show the ^{1}H NMR spectra of tung oil-derives and CTMA, which have been used to determine the copolymer composition. In the ^{1}H NMR spectrum of CTMA, the proton resonances of –COOCH$_3$ (3.69 ppm) in METOFA and –CH$_3$ (0.91 ppm) in TOFA and METOFA are well separated, whereas those

for methylene protons and methine protons (1–2.5 ppm) are overlapped. Hence, their relative peak areas can be used to calculate the mole fraction of the monomer by the following formulas,

$$F(\mathrm{AN}) = \frac{\left(B - \dfrac{A}{3} \times 22\right)\Big/ 3}{\dfrac{A}{3} + \left(B - \dfrac{A}{3} \times 22\right)\Big/ 3} \tag{1}$$

$$F(\mathrm{METOFA}) = \frac{C/3}{\dfrac{A}{3} + \left(B - \dfrac{A}{3} \times 22\right)\Big/ 3} \tag{2}$$

$$F(\mathrm{TOFA}) = \frac{(A - C)/3}{\dfrac{A}{3} + \left(B - \dfrac{A}{3} \times 22\right)\Big/ 3} \tag{3}$$

where A and C are the peak areas for the proton resonances of –CH$_3$ and –COOCH$_3$, respectively. B is the peak area for all the methylene proton and methine proton resonances, which include those of the tung oil derive and acrylonitrile. F (AN), F (METOFA) and F (TOFA) correspond to the mole fraction of AN, METOFA and TOFA, respectively. The calculation results are presented in Table 1.

Differential scanning calorimetry

Fig. 6 shows the results of DSC. In Fig. 6(a), we can observe a melting peak and a crystallization peak, which illustrates the crystallizability of CTMA. Moreover, the approximate enthalpy values confirm the corresponding melt crystallization process. As observed in the CTMA structure shown in Fig. 1, the flexibility of the long aliphatic chain causes the molecules to align; this leads to crystallization. Furthermore, the induction forces induced by the cyano groups were able to stabilize the crystallization. Note that *via* both the heating curve and the cooling curve, the glass transition temperature of CTMA can be detected, which is around −26.76 °C.

However, no melting or crystallization peaks were observed in the curves of E-CTMA, and only one glass transition temperature could be detected, which indicated that no phase separation occurred. This was because the epoxy resin incorporated CTMA by the reaction between the carboxyl groups and the epoxy groups; this contributed to the molecular-level compatibility.

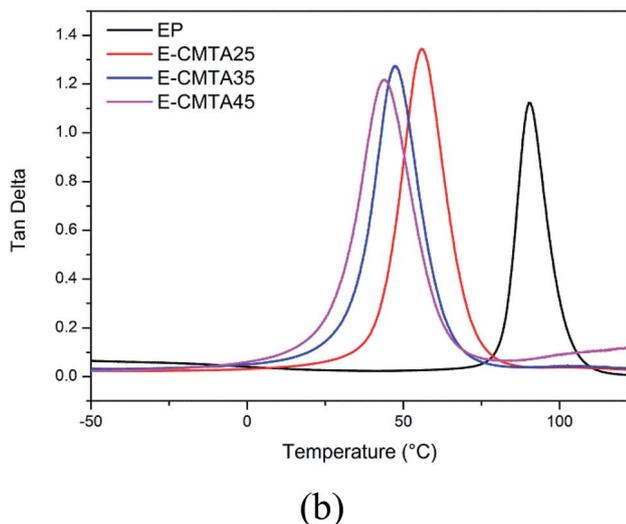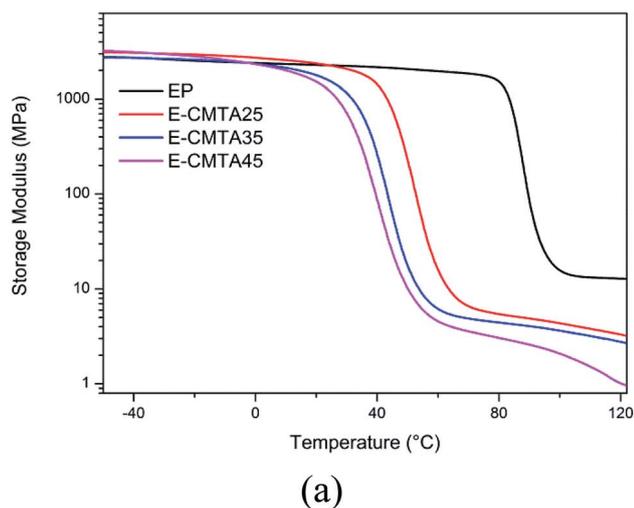As flexible cross-linkers, many long flexible aliphatic chains were incorporated into E-CTMA thermosets. Segment

Fig. 8 Storage modulus (a) and tan δ (b) of the neat epoxy resin and E-CTMA thermosets.

Table 3 DMA results of the neat epoxy resin and E-CTMA thermosets

Sample code	T_g (°C)	Half-peak width (°C)	E'^a	v_e (10^{-3} mol cm^{-3})
EP	90.15	11.12	12.86	1.31
E-CTMA25	55.75	16.27	5.10	0.57
E-CTMA35	47.38	16.88	4.53	0.52
E-CTMA45	43.77	19.93	3.36	0.39

^{a} Storage modulus at T_g + 30 °C.

movement in flexible aliphatic chains can be easily induced by increasing the temperature, which will contribute to a lower glass transition temperature; furthermore, the high cross-linking network system will be destroyed, and the less restriction from covalent bonds contributes to segment movement, which will also contribute to a lower glass transition temperature. All these results are in accordance with the decreasing T_g value shown in Fig. 6(b); moreover, further explanation about this point has been provided in the discussion of DMA.

Furthermore, the curing behavior was studied by DSC. In Fig. 7(a), all samples show a similar curing behavior, and only one curing process has been determined. The accurate parameters of the curing process are presented in Table 2. Obviously, the T_o and T_p values of E-CTMAs are significantly lower than that of the neat epoxy resin, and a decreasing tendency is observed as the content of CTMA is increased. Previous studies have demonstrated that the existence of strong hydrogen bonding species, such as acids and alcohols, is able to accelerate the epoxy–amine reaction.[25] In the blending process, the carboxyl groups in CTMA react with the epoxy groups, and the same amount of hydroxyls are simultaneously produced. Therefore, the curing process is accelerated, which is in agreement with the decreased values of T_o and T_p. Furthermore, this positive effect on the curing process is shown in Fig. 7(b) in which it is observed that CTMA enhances the conversion at a specific temperature; however, higher content of CTMA results in lower enthalpy (ΔH). This is because the addition of CTMA reduces the content of epoxy groups and curing agent; this leads

to fewer reactions. Moreover, the incorporation of CTMA increases the viscosity of epoxy resin (Table 2), which is attributed to the much higher molecular weight of CTMA. Furthermore, the pre-reaction between the carboxyl and the epoxy groups may produce hydroxyls, which may form hydrogen bonds with other polar groups and further increase the viscosity. Similar results have been obtained in previous studies, in which rubber and other oil-based polymers have been used to toughen the epoxy resin.[12,21,26] The increased viscosity may restrict the movement of reaction groups and then reduce the enthalpy.

Dynamic mechanical analysis

Fig. 8 shows the temperature dependence of storage modulus and tan δ of the neat epoxy resin and E-CTMA thermosets. The accurate statistics of thermal properties are presented in Table 3.

T_g decreases with an increase in the CTMA content; this is in accordance with the abovementioned DSC results provided in the DSC section. Furthermore, the explanation of the decreasing T_g can be confirmed by the results of half-peak width (HPW) in tan δ curves, which is related to structural uniformity.[27] The neat epoxy resin has the lowest HPW value, whereas E-CTMA45 has the highest HPW value of E-CTMA. This is because CTMA acts as a flexible crosslinker, which increases the molecular weight between cross-linking points. Furthermore, the random carboxyl distribution of CTMA extends the
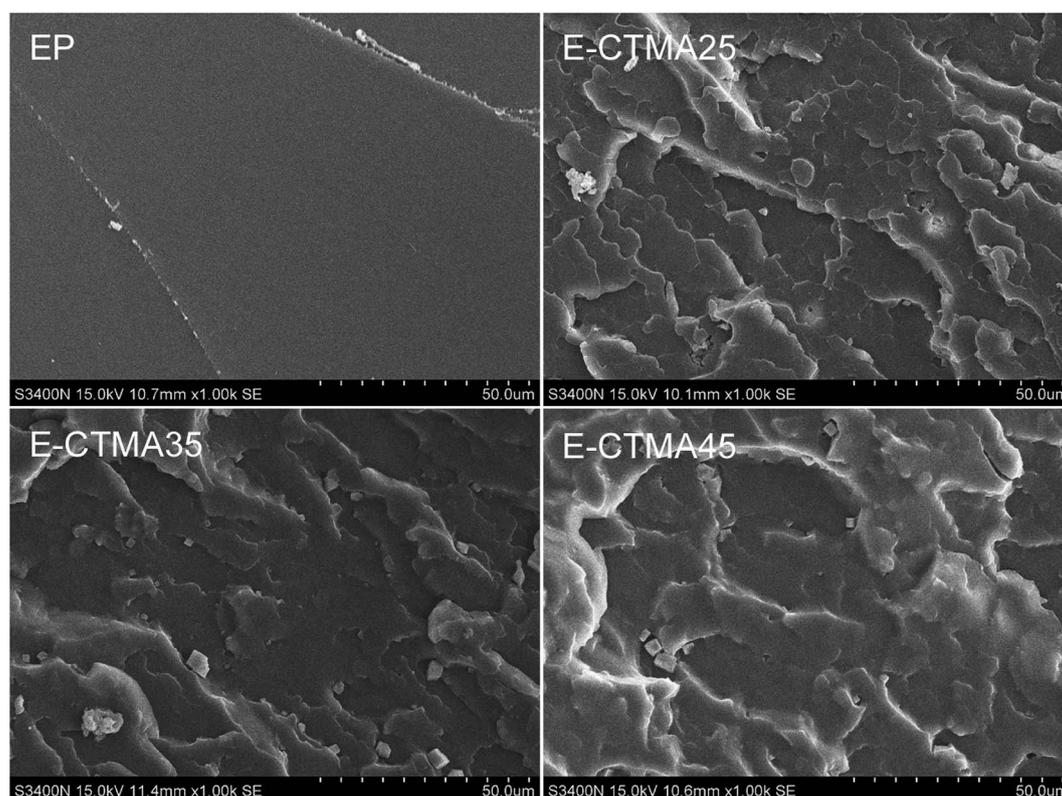

Fig. 9 SEM images of the frozen fracture morphology for the thermosets: neat epoxy, E-CTMA25, E-CTMA35 and E-CTMA45.

dispersity of molecular weight between cross-linking points. However, every tan δ curve of E-CTMAs and neat epoxy resin has only one peak, which illustrates that the uniform network structure is unable to lead to phase separation.[28,29]

Based on the theory of rubber elasticity, the cross-linking density v_e can be calculated from the storage modulus in the rubbery region:

$$v_e = \frac{E'}{3RT} \qquad (4)$$

where E' is the storage modulus at $T_g + 30\ °C$, R is the gas constant, and T is the absolute temperature at $T_g + 30\ °C$.[14,24]

The value of v_e decreases with the increasing content of CTMA; this indicates lower cross-linking density. With fewer cross-linking points, chain segments move more easily; this contributes to a lower glass transition temperature. Thus, the decreasing glass transition temperatures are presented as T_g value in Table 3.

Morphology of the fractured surfaces

In the SEM images shown in Fig. 9, we can observe that the fracture surface of neat epoxy samples is very smooth, whereas that of the CTMA-modified epoxy samples is rather rough. No cavity was observed on the fracture surfaces; this indicated that no phase separation occurred.[14,30] This result is in line with the results of DSC and DMA. Furthermore, massive shear yields and plastic deformations observed on the E-CTMA fracture surfaces indicate a typical toughness character.

When CTMA was added as a modifier, the carboxyl groups reacted with the epoxy groups; this led to molecular level incorporation instead of phase separation. This phenomenon has also been observed by other researchers.[31–34] Because of the long aliphatic chains of CTMA, external stresses can be redistributed, and plastic deformations will be induced by the flexible cross-linker. This is the reason why the fracture surfaces become rougher.

Thermogravimetric analysis

The thermal stability of CTMA and the neat epoxy resin and E-CTMA thermosets was examined, as shown in Fig. 10. We can observe that E-CTMAs tend to decompose at lower temperatures, $T_{5\%}$ and $T_{10\%}$ presented in Table 4; this is attributed to the decomposition of small molecules (carbonyl and ester) in CTMA. Consequently, a subtle peak at 250 °C appears in the derivative curves with an increase in CTMA content, which has been magnified in the inset of Fig. 10(b). The peak around 395 °C in the derivative curves demonstrates the main decomposition process, which is considered to be caused by the degradation of the cross-linked epoxy resin networks.[35,36] Hence, the maximum degradation rate temperatures of E-CTMA and neat epoxy resin thermosets are approximate. Similar results have been reported by other researches.[35,37–39] Kumar et al. toughened the epoxy resin using ESO in different contents, and the results show that $T_{5\%}$ decreases from 341 °C to 283 °C when the mass ratio between epoxy resin and ESO is 80/20;[38] however, CTMA leads to a greater weight loss; this may be
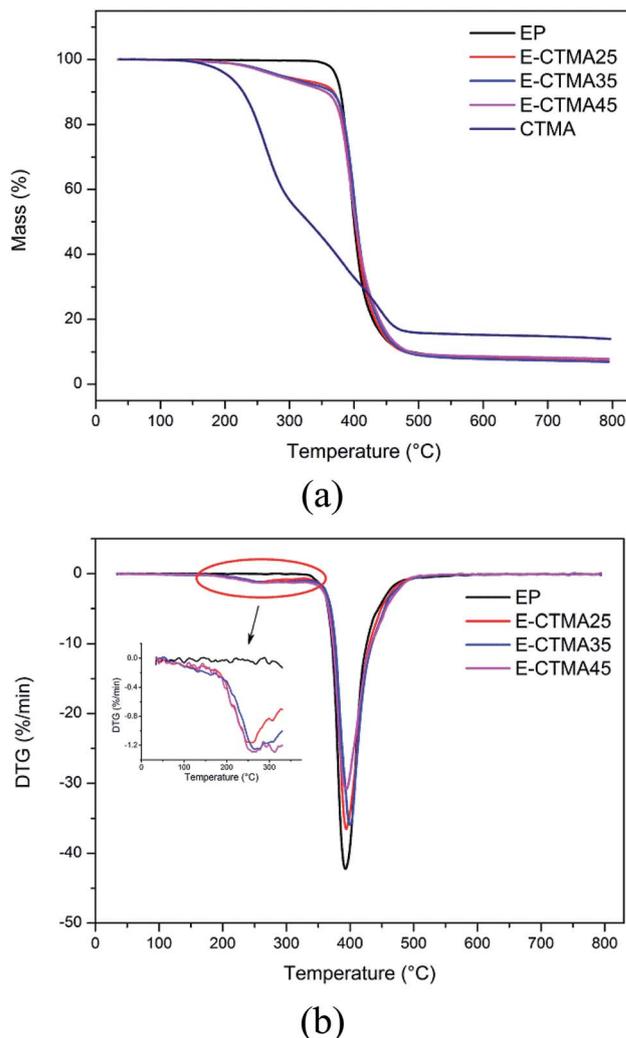

(a)

(b)

Fig. 10 Thermogravimetric plots of the curing system: TG curves (a) and DTG curves (b).

explained in terms of the cross-linking density. As is well-known, higher cross-linking density contributes to higher thermal stability.[38] The incorporation of CTMA results in a great loss in the cross-linking density, which may account for the loss in thermal stability. However, the epoxide equivalent weight of

Table 4 Thermal properties of the neat epoxy resin and E-CTMA thermosets

Sample code	$T_{5\%}^{a}$ (°C)	$T_{10\%}^{a}$ (°C)	T_m^{b} (°C)
EP	372.06	378.92	392.7
E-CTMA25	286.11	368.04	394.0
E-CTMA35	285.91	365.29	400.2
E-CTMA45	279.49	355.32	393.8
CTMA	204.94	227.84	263.9

[a] $T_{5\%}$ and $T_{10\%}$ are the temperatures of 5% and 10% weight loss, respectively. [b] T_m is the temperature at which the degradation rate is maximum.
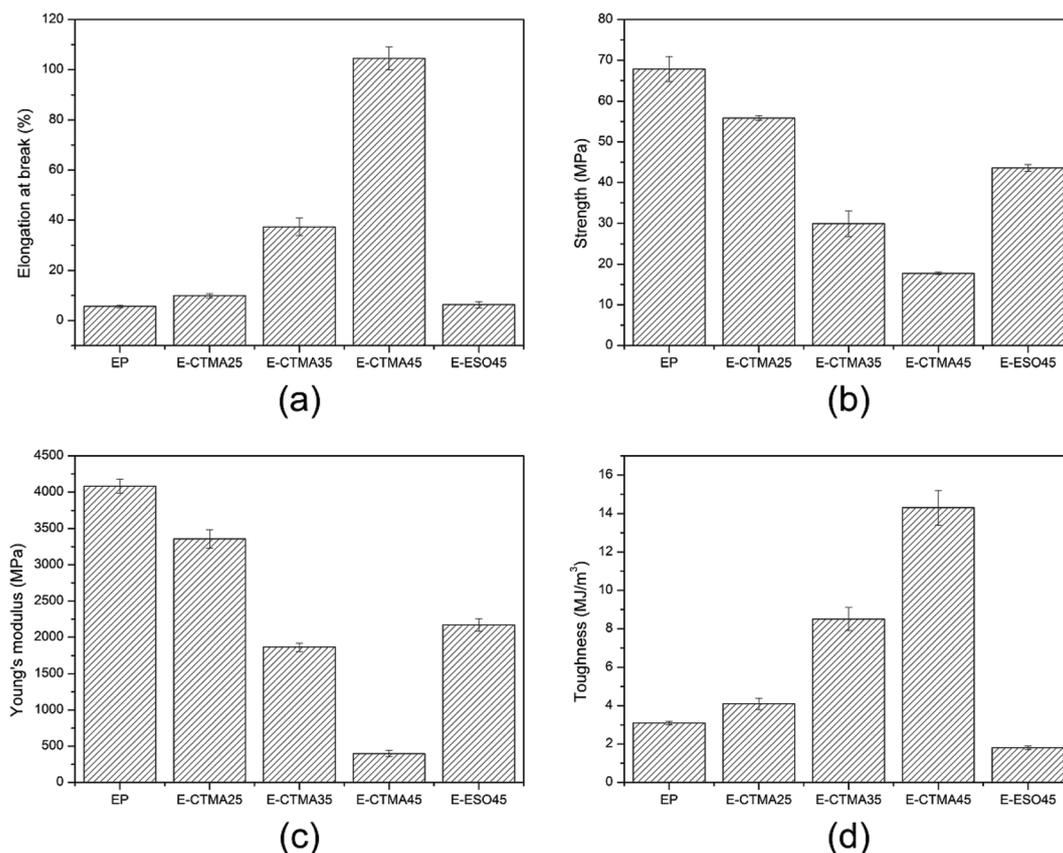
Fig. 11 Mechanical properties of the neat epoxy resin and E–CTMA thermosets.

commercial ESO is about 260 g mol^{-1}. In other words, each ESO molecule contains more than 3 epoxy groups on an average, which may react with the curing agent and avoid a sharp decrement in the cross-linking density. Therefore, the reduction of thermal stability is less.[35]

Mechanical properties

The mechanical properties of all thermosets are shown in Fig. 11. As can be seen, the elongation-at-break, which indicates the toughness of the material, has increased dramatically from 5.6% to 104.5%; this suggests that CTMA can effectively toughen the epoxy curing system. This is owing to the flexibility of the modifier, which may restrict crack extension and induce crazes.[40] Compared with other tung oil-based products synthesized by the Diels–Alder reaction, whose elongation-at-break is less than 5%, E-CTMAs show higher toughness.[21,23,24] However, an increase in the content of CTMA decreases the tensile strength and Young's modulus. Because the addition of CTMA reduces the cross-linking density and enhances ductility, the modified samples are less sensitive to deformation; this leads to lower Young's modulus.[41,42] In addition, due to the presence of less covalent bonds, the samples are unable to withstand high stress; this accounts for the decrement of tensile strength. Furthermore, toughness can be indicated in terms of fracture energy. The increasing toughness, calculated by integrating the area under stress–strain curves,[43] demonstrates that CTMA can effectively toughen the epoxy curing system as well.

The sample E-ESO45 was used for comparison. Obviously, although E-ESO45 has higher tensile strength and Young's modulus, its toughness value is much lower than that of E-CTMA45; this is mainly attributed to its low elongation-at-break. Moreover, many studies on the toughening of epoxy resin with ESO have been reported, which indicate that ESO shows limited improvement in the elongation-at-break.[20,35,38,39] Hence, in terms of elongation-at-break and toughness value, CTMA exhibits excellent toughening ability, which is better than ESO. Moreover, the mechanical properties suggest that the epoxy resin modified by CTMA is a potential material that can be used as a coating, pouring sealant and other casting material and has higher requirement for toughness but less demand for strength.[44] However, owing to the higher viscosity of some formulations, some solvents should be used to reduce the viscosity for applications.

Conclusions

Epoxy resin modified by CTMA shows a great improvement in toughness when compared with the neat epoxy resin and the sample modified by ESO. By acting as a flexible cross-linker, CTMA reduces the cross-linking density of epoxy resin, simultaneously increasing the elongation-at-break and toughness

value. However, the incorporation of flexible aliphatic chains decreases the tensile strength, Young's modulus and T_g value; this is similar to the results of rubber-modified epoxy resin. Due to the reaction between the carboxyl groups and the epoxy groups, no phase separation has been detected by thermal characterization and SEM. Based on these characteristics, the epoxy resin modified by CTMA is a potential material for application as a coating, pouring sealant and casting material; moreover, the results demonstrate that the modified resins obtained from renewable feedstock, such as tung oil, will be potential alternatives to petroleum-based modified resins in the future.

Conflicts of interest

There is no conflict of interest to declare.

Acknowledgements

References

1 Y. Huang, Y. Tian, Y. Li, X. Tan, Q. Li, J. Cheng and J. Zhang, *RSC Adv.*, 2017, **7**, 49074–49082.
2 R. Pearson and A. Yee, *J. Mater. Sci.*, 1989, **24**, 2571–2580.
3 A. F. Yee and R. A. Pearson, *J. Mater. Sci.*, 1986, **21**, 2462–2474.
4 H. Ren, X. Zhan, Q. Zhang and F. Chen, *RSC Adv.*, 2016, **6**, 35621–35627.
5 H. Ren, X. Zhan, Q. Zhang and F. Chen, *J. Appl. Polym. Sci.*, 2016, **133**, 42826.
6 X. Fernández-Francos, D. Foix, À. Serra, J. M. Salla and X. Ramis, *React. Funct. Polym.*, 2010, **70**, 798–806.
7 M. Flores, X. Fernández-Francos, F. Ferrando, X. Ramis and À. Serra, *Polymer*, 2012, **53**, 5232–5241.
8 X. Fei, W. Wei, Y. Tang, Y. Zhu, J. Luo, M. Chen and X. Liu, *Eur. Polym. J.*, 2017, **90**, 431–441.
9 D. Foix, A. Serra, L. Amparore and M. Sangermano, *Polymer*, 2012, **53**, 3084–3088.
10 L. Calabrese and A. Valenza, *Eur. Polym. J.*, 2003, **39**, 1355–1363.
11 K. Srivastava, A. K. Rathore and D. Srivastava, *Spectrochim. Acta, Part A*, 2018, **188**, 99–105.
12 J. Xi and Z. Yu, *J. Appl. Polym. Sci.*, 2018, **135**, 45767.
13 L. Hader-Kregl, G. M. Wallner, R. W. Lang and B. Strauß, *J. Appl. Polym. Sci.*, 2018, **135**, 46094.
14 J. Huang and X. Nie, *Polym. Int.*, 2016, **65**, 835–840.
15 R. J. Day, P. A. Lovell and A. A. Wazzan, *Polym. Int.*, 2001, **50**, 849–857.
16 G. M. Roudsari, A. K. Mohanty and M. Misra, *ACS Sustainable Chem. Eng.*, 2017, **5**, 9528–9541.

17 S. Miao, P. Wang, Z. Su and S. Zhang, *Acta Biomater.*, 2014, **10**, 1692–1704.
18 S. Qureshi, J. A. Manson, J. C. Michel, R. W. Hertzberg and L. H. Sperling, in *Characterization of Highly Cross-linked Polymers*, American Chemical Society, 1984, vol. 243, ch. 8, pp. 109–124.
19 H. Miyagawa, A. K. Mohanty, M. Misra and L. T. Drzal, *Macromol. Mater. Eng.*, 2004, **289**, 636–641.
20 D. Ratna, *Polym. Int.*, 2015, **50**, 179–184.
21 K. Huang, J. Xia, X. Yang, M. Li and H. Ding, *Polym. J.*, 2010, **42**, 51–57.
22 L. Hou and Y. Liu, *J. Appl. Polym. Sci.*, 2012, **126**, 1572–1579.
23 K. Huang, Z. Liu, J. Zhang, S. Li, M. Li, J. Xia and Y. Zhou, *Biomacromolecules*, 2014, **15**, 837–843.
24 K. Huang, P. Zhang, J. Zhang, S. Li, M. Li, J. Xia and Y. Zhou, *Green Chem.*, 2013, **15**, 2466–2475.
25 J. M. Barton, *The application of differential scanning calorimetry (DSC) to the study of epoxy resin curing reactions*, 1985.
26 A. Saikia and N. Karak, *Polym. Degrad. Stab.*, 2017, **135**, 8–17.
27 A. R. Kannurpatti, J. W. Anseth and C. N. Bowman, *Polymer*, 1998, **39**, 2507–2513.
28 L. Wang, Y. Liang, Q. Yu, S. Chen, J. Zhang, M. Miao and D. Zhang, *Polym. Compos.*, 2018, **39**, 2046–2055.
29 X. Miao, Y. Meng and X. Li, *Polymer*, 2015, **60**, 88–95.
30 L. Lijuan, M. Yan, Q. Teng, L. Zhuoxin, Y. Jing, C. Xingzhong and L. Xiaoyu, *Polym. Compos.*, 2013, **34**, 1051–1060.
31 T. Li, H. Qin, Y. Liu, X. Zhong, Y. Yu and A. Serra, *Polymer*, 2012, **53**, 5864–5872.
32 J.-P. Yang, Z.-K. Chen, G. Yang, S.-Y. Fu and L. Ye, *Polymer*, 2008, **49**, 3168–3175.
33 M. Morell, M. Erber, X. Ramis, F. Ferrando, B. Voit and A. Serra, *Eur. Polym. J.*, 2010, **46**, 1498–1509.
34 L. Luo, T. Qiu, Y. Meng, L. Guo, J. Yang, Z. Li, X. Cao and X. Li, *RSC Adv.*, 2013, **3**, 14509–14520.
35 S. K. Sahoo, S. Mohanty and S. K. Nayak, *RSC Adv.*, 2015, **5**, 13674–13691.
36 P. Chand, C. V. Reddy, J. G. Verkade, T. Wang and D. Grewell, *Energy Fuels*, 2009, **23**, 989–992.
37 C. Yan, L. Yang, L. Ma, D. E. Finlow, S. Lin and K. Song, *J. Therm. Anal. Calorim.*, 2013, **113**, 939–945.
38 S. Kumar, S. K. Samal, S. Mohanty and S. K. Nayak, *Ind. Eng. Chem. Res.*, 2017, **56**, 687–698.
39 S. K. Sahoo, S. Mohanty and S. K. Nayak, *Chin. J. Polym. Sci.*, 2015, **33**, 137–152.
40 J. M. Misasi, Q. Jin, K. M. Knauer, S. E. Morgan and J. S. Wiggins, *Polymer*, 2017, **117**, 54–63.
41 H. Ren, X. Zhan, Q. Zhang, G. Zhang and F. Chen, *Polymer*, 2016, **92**, 222–230.
42 H. Ren, X. Zhan, Q. Zhang and F. Chen, *J. Appl. Polym. Sci.*, 2017, **134**, 44849.
43 J. Song, C. Chen, S. Zhu, M. Zhu, J. Dai, U. Ray, Y. Li, Y. Kuang, Y. Li and N. Quispe, *Nature*, 2018, **554**, 224–239.
44 L. Ying and S. Mao, *J. Appl. Polym. Sci.*, 1996, **61**, 2059–2063.